Published in PASP
Preprint typeset using LaTeX style emulateapj v. 5/2/11

THE λ108300 HE I ABSORPTION LINE AMONG METAL-POOR SUBDWARFS

Graeme H. Smith
University of California ObservatoriesLick Observatory, Department of Astronomy & Astrophysics, UC Santa Cruz, 1156 High St., Santa Cruz, CA 95064, USA

Andrea K. Dupree
Harvard-Smithsonian Center for Astrophysics, Cambridge, MA 02138, USA

Jay Strader
Department of Physics and Astronomy, Michigan State University, East Lansing, MI 48824, USA
Published in PASP

ABSTRACT

Spectra of the He I λ10830 line have been obtained for 23 metal-poor stars, the majority of which are dwarfs ranging in metallicity from $-2.1 \leq$ [Fe/H] ≤ -0.8. The data were acquired with the NIRSPEC spectrograph on the Keck 2 telescope. Most of these subdwarfs and dwarfs are found to exhibit a He I absorption line indicative of the presence of chromospheres. The equivalent width of the λ10830 absorption profile is generally less than 70 mÅ, and covers a range similar to that found in solar metallicity stars of low activity. Among the subdwarfs the λ10830 equivalent width does not correlate with either [Fe/H] metallicity or $(B-V)$ color. Some evidence for asymmetric profiles is found among metal-poor dwarfs, but not the high-speed blue-shifted absorption displayed by some metal-poor red giants.

Subject headings: Stars

1. INTRODUCTION

Whereas chromospheres are known to be present among both metal-poor Population II subdwarfs (Peterson & Schrijver 1997; Smith & Churchill 1998; Takeda & Takada-Hidai 2011) and giants (Dupree et al. 1990, 2007; Dupree & Smith 1995; Smith & Dupree 1998; Cacciari et al. 2004; Mauas et al. 2006; Mészáros et al. 2009; Smith et al. 1992; Vieytes et al. 2011) despite their great age, and whereas the He I triplet line at 10830 Å can serve as a tracer of chromospheric conditions among Luminosity Class V and III F-G-K stars (Zirin 1982; O'Brien & Lambert 1986; Zarro & Zirin 1986; Shcherbakov & Shcherbakova 1991; Andretta & Giampapa 1995; Sanz-Forcada & Dupree 2008), and reveal mass motions of quite high velocity among red giants (O'Brien & Lambert 1986), and whereas the profiles of the He I 10830 Å line have been found to exhibit evidence of fast outflows among metal-poor red giants (Dupree et al. 1992, 2009; Smith et al. 2004), it seems warranted to document the behavior of the He I 10830 Å profile among metal-poor dwarf and subdwarf stars. If the fast outflows found among some metal-poor red giant branch (RGB) and red horizontal branch (RHB) stars (Dupree et al. 2009) are to be associated with mass loss that uniquely occurs during the red giant phase of evolution then one might not expect evidence of them among subdwarf stars. On the other hand, if the He I fast outflows carry very minor amounts of mass and prove to be commonplace among the upper atmospheres of late-type stars of widely differing surface gravity and luminosity, then it may be concluded that they are of no significance in the mass loss history of Population II red giants. It is to address this issue that we report upon below the results of a spectroscopic survey of the He I line for a sample of metal-poor dwarf stars that was carried out with the NIRSPEC spectrometer on the Keck 2 telescope. A comparable program of similar scope has previously been published by Takeda & Takada-Hidai (2011) using the Subaru telescope. Our surveys prove to be largely complementary and there is only modest overlap in the stars observed in these two programs.

graeme@ucolick.org
dupree@cfa.harvard.edu
strader@pa.msu.edu

2. OBSERVATIONS

A selection of metal-poor halo dwarf stars was observed over the course of $1\frac{1}{2}$ nights in November 2009 using the NIRSPEC spectrograph (McLean et al. 2000) on the Keck 2 telescope. The stars reported upon in this paper were chosen from the *Catalogue of [Fe/H] Determinations of F, G, K stars* compiled by Cayrel de Strobel et al. (2001). They were selected from among those stars for which at least one published abundance measurement yielded a result of [Fe/H] < -0.8. The stars were also listed as being of luminosity class V or IV in the Cayrel de Strobel et al. (2001) catalogue.

The program stars are listed in Table 1. Photometry in columns 3 and 4 of the table is taken from *The General Catalogue of Photometric Data* (Mermilliod et al. 1997) where available, for a few stars these values are taken from the *Hipparcos Catalog* (ESA 1997). Parallaxes (column 5) in most cases are also taken from the Hipparcos Catalog, but from Lepine (2007) in the case of HD 23439B. Absolute magnitudes in column 6 have been computed without any attempt to correct for possible interstellar absorption along the line of sight. Spectroscopic

metallicities for each star are listed in Table 1 (column 7) together with a note of the references (column 8) from which the values of [Fe/H] were obtained. In several cases where there is some dispersion in the literature measurements two values of [Fe/H] are listed. Radial velocities v_r as taken from the SIMBAD data base are listed in column 9 of Table 1. Of the stars in our sample HD 194598 and HD 201891 were also observed by Takeda & Takada-Hidai (2011).

Observations were made on the night of 2009 November 22 UT and the first half of the night of November 23 UT. NIRSPEC (McLean et al. 1998) was used in high-resolution mode with the NIRSPEC-1 above-slit filter and echelle and cross-disperser angles chosen so as to place the wavelength range from 0.95 to 1.12 μm on the ALADDIN-3 1024×1024 detector (which has 27 μm pixels). The 1.083 μm He I line is located within order 70. The thin blocking filter which is available with NIRSPEC to reduce longer-wavelength thermal leakage was not used in these observations due to concern that it would introduce fringing into the spectra on wavelength scales comparable to the width of the stellar He I line. A 0.43×12 arsec slit was used in all observations.

The total exposure time allocated to each star is listed in column 2 of Table 1 as the product of three factors that define how each observation was carried out. The first digit is the number of nod points at which integrations were performed, it is either 2 (for an AB nod pattern) or 4 (for an ABBA pattern). The second digit is the number of coadded integrations made at each nod position and the third digit gives the integration time in seconds per coadd. The only star that was observed with an ABBA nod pattern is HD 194598, the other stars in Table 1 were observed in an AB nod pair. In the instances of HD 31128 and HD 76932 two AB nod pairs were performed, and the integration times per coadd for each pair are listed in brackets.

Observations of a variety of hot rapidly-rotating bright stars were interspersed throughout the night for monitoring telluric absorption features. Spectra of flat field lamps and NeArKr comparison arcs were also obtained at the beginning and end of 22 November, and at the beginning of the 23 November half-night. A spectrum of a K giant was used to verify the dispersion relation.

3. RESULTS

The (M_V, $B-V$) color-magnitude diagram (CMD) of the stars from Table 1 is shown in Figure 1. The $B-V$ colors plotted are the observed colors, no correction has been made for interstellar reddening. As a precedent, Gratton et al. (2000) assumed that metal-poor dwarfs in their abundance survey, which includes a number of stars in Table 1, had negligible reddening. They considered this assumption to be reasonable "in view of their small distances." A large fraction of the stars in Table 1 are included in a re-analysis of the Geneva-Copenhagen survey of solar neighborhood dwarf stars performed by Casagrande et al. (2011). For most of these stars the reddening in their catalog is quoted as $E(B-V) = 0.00$. Only in one case is a small non-zero reddening given by them, namely, HD 97916 ($E(B-V) = 0.025$).[1] Those

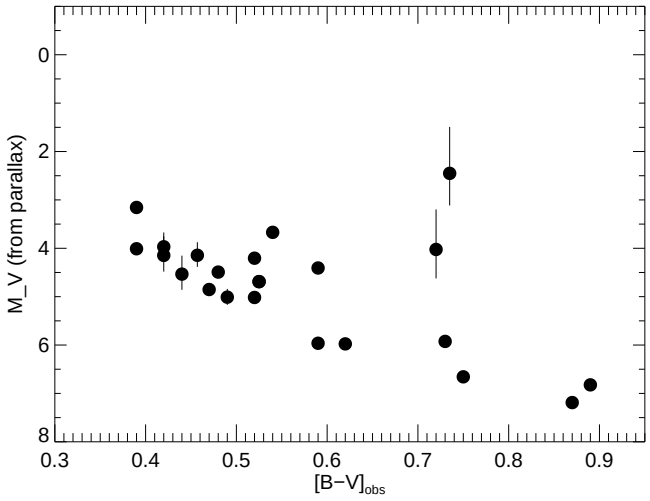

Figure 1. The (M_V, $B-V$) color-magnitude diagram of stars with He I spectra listed in Table 1. The error bars on the absolute magnitude are derived from the uncertainties in the *Hipparcos* parallaxes. In most cases the error bars are smaller than the diameter of the plotted points.

program stars with $M_V > +3.0$ fall at locations in the CMD that are consistent with them being dwarfs. HD 3179 with $M_V \sim +2.5$ falls near the base of the red giant branch and could be classified as a subgiant.

The spectra were reduced using the IDL package REDSPEC[2] McLean et al. (2003), as described in Dupree et al. (2009). Spectra were normalized by a continuum that was derived using a cubic spline fit to the line-free portions of the data.

The spectrum of each star in Table 1 derived from the NIRSPEC order containing the λ10830 He I line is shown in one of the various panels of Figure 2(a-b). The wavelength scale of each panel corresponds to the rest frame of the metal-poor star plotted in that panel. Several rapidly rotating hot stars were observed throughout the night to document the pattern of telluric water vapor absorption lines in the NIRSPEC order containing the stellar He I line. One of these hot star spectra is plotted in each of the panels of Figure 2, shifted in wavelength so as to match the rest frame of each star. Comparison between the metal-poor and hot star spectra in each panel allow the telluric lines to be identified in each metal-poor star spectrum.

The properties of the He I line that are of interest here are the strength of the absorption plus the possibility of any profile asymmetry that might be indicative of mass motions in the outer atmosphere. The spectra of the stars in our program are further presented in Figure 3(a-b) in a higher resolution version that shows a limited wavelength region (10820 to 10835 Å) near the Si I and He I transitions. The spectra are aligned on the strong Si I 10827.1 Å transition. The location of any potential He I line is marked in each panel together with a strong line of Si I. Telluric features can be identified by comparison with Figure 2.

The equivalent width (EW) of each He I line was mea-

[1] Stars from Table 1 not included in Casagrande et al. (2011) are HD 3567, HD 7424, HD 16031, HD 23439B, HD 194598.

[2] `http://www2.keck.hawaii.edu/inst/nirspec/redspec.html`

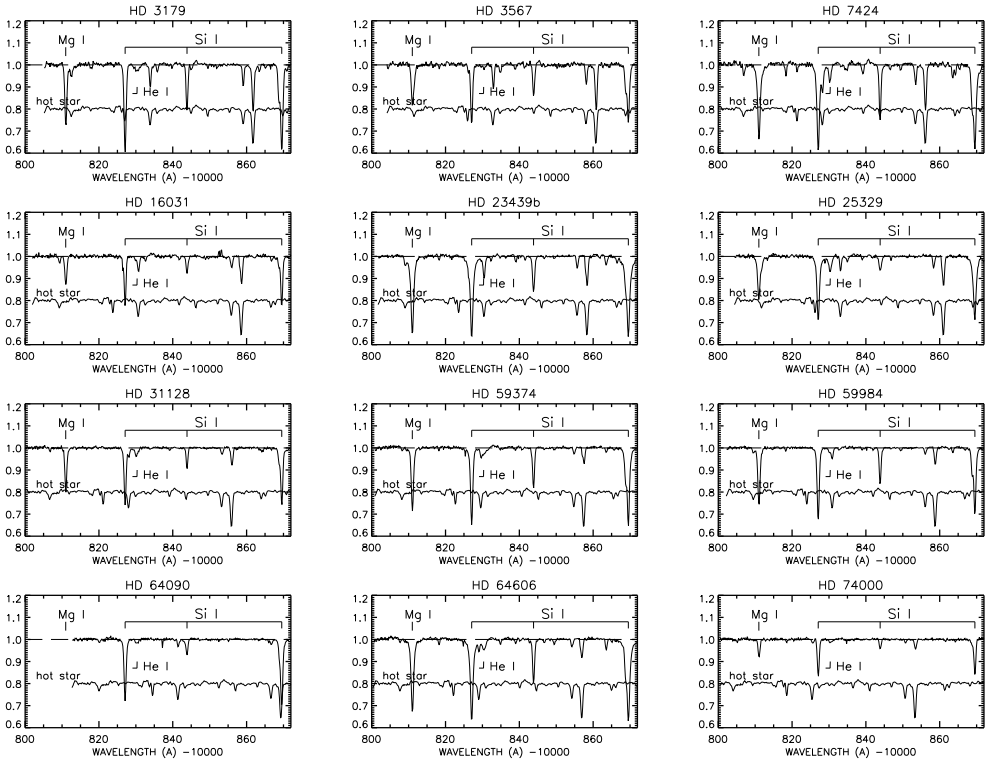

Figure 2a. Figure 2a. See caption below.

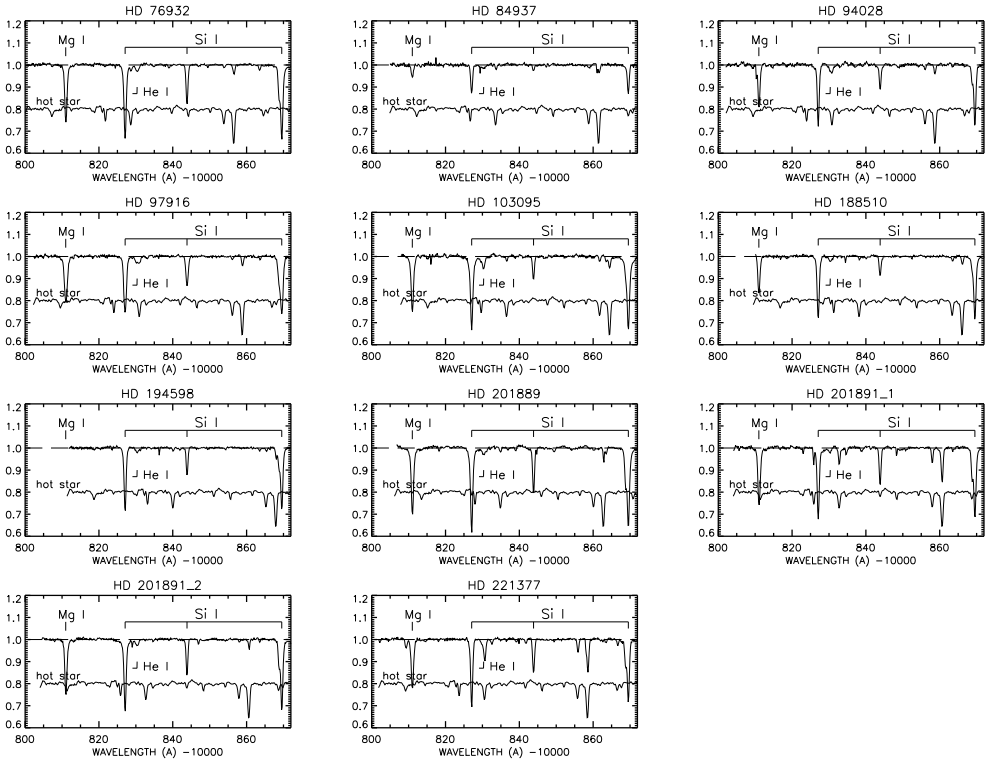

Figure 2b. Spectra of the wavelength range λ10800-10870 for metal-poor stars listed in Table 1, with the stellar absorption lines of He I, Mg I and Si I marked. In each panel the spectrum of a hot star is also shown that is shifted in wavelength so that the telluric lines match the positions of those in the subdwarf spectrum. The 'hot star' shows a typical water vapor spectrum and is the same for all panels, it is not scaled to the amount of water vapor in the spectrum of the metal-poor star in each panel. All spectra have been normalized by the local continuum, and the hot star spectrum is shifted vertically by an arbitrary amount. The wavelength scale is that of the rest frame of the metal-poor star.

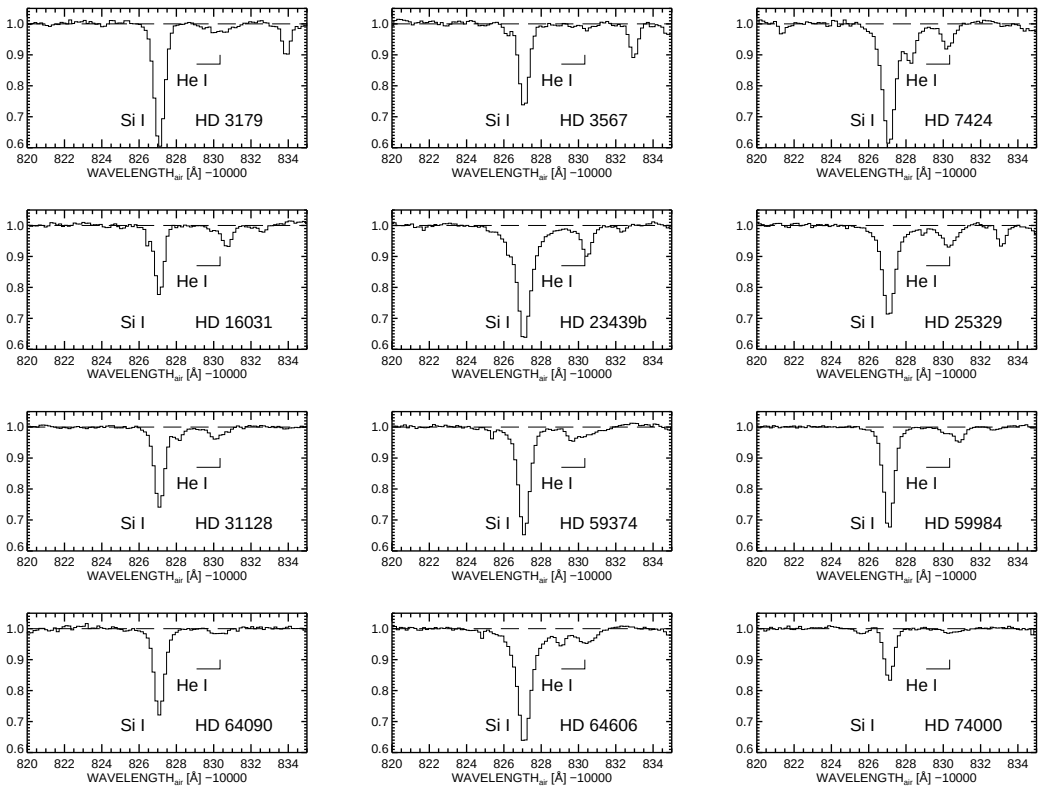

Figure 3a. Figure 3a. See caption below.

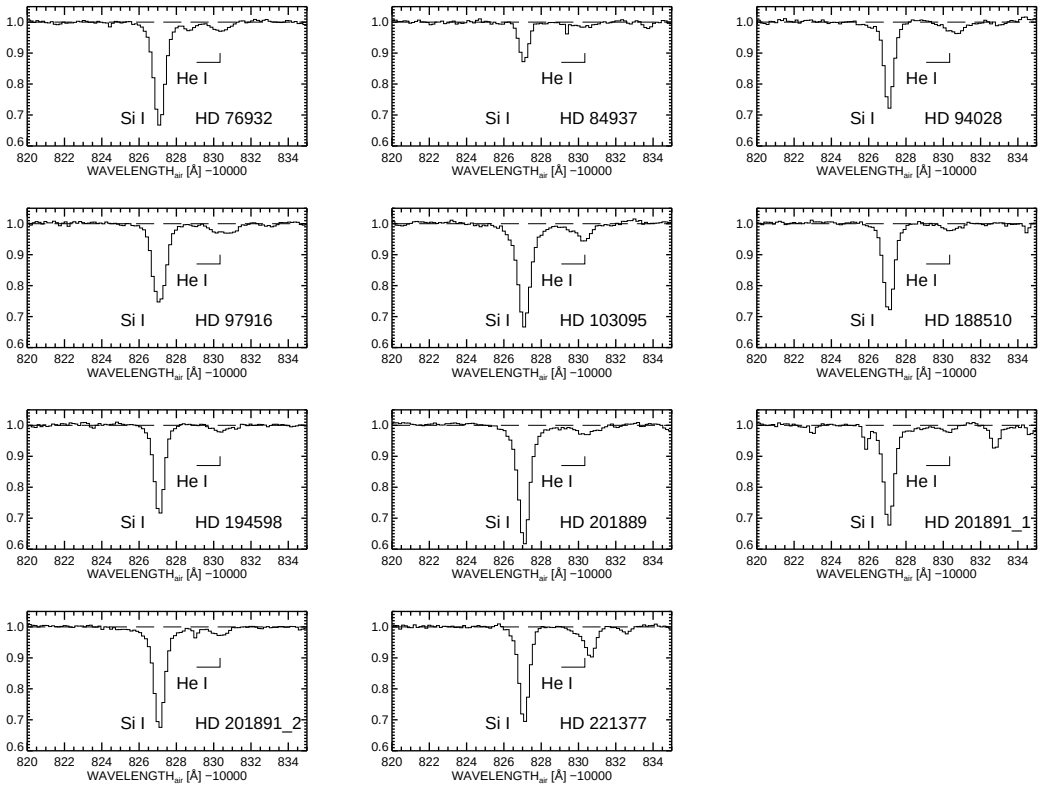

Figure 3b. Spectra of the λ10830 He I line (normalized to a local continuum) for metal-poor stars listed in Table 1. Each spectrum is plotted in the stellar rest frame.

sured using the `splot` option within the IRAF software package[3] by direct integration of the continuum normalized profile. In instances where telluric water vapor intervened close to, but separable from, the He I line, deblending of the wavelength region containing the Si I, H_2O, and He I features was carried out by simultaneously fitting the profiles of all three features. Another complication can be the presence of a Ti I line 10828.04 Å in the coolest stars; by contrast the strongest helium line component is at 10830.34 Å and the weakest of the triplet is at 10829.08 Å, such that the Ti I line may blend with the He I profile.

The field stars in Table 1 have a range of radial velocity. There is one substantial water vapor line at a terrestrial rest wavelength near 10832 Å in the vicinity of the Si I and He I lines. This telluric feature can be identified, for example, in Figure 2 between the Si I and He I lines in the spectra of HD 7424, HD 31128, HD 64606, and HD 76932. These stars have radial velocities of 85-121 km s^{-1}. Over the course of our 1.5-night observing run the He I *EW*s of stars with radial velocities in the range $v_r \sim$ 30-80 km s^{-1} were susceptible to overlap with the λ10832 telluric line. As noted above, several hot stars were observed to measure a telluric spectrum. However, rather than use hot-star spectra as telluric templates to divide into the object spectrum we adopt a technique analogous to that employed by Dupree et al. (2011) to correct the He I *EW*s for telluric absorption when necessary. There is another strong telluric feature in the vicinity of λ10860, and for many of the metal-poor star spectra the equivalent width of both this feature and the λ10832 telluric line can be cleanly measured. Similar measurements were made from the hot star spectra obtained at various airmasses during the run. Figure 4 shows that there is a correlation between the equivalent widths of these two telluric features, and the solid line shows a linear least squares fit which has the equation $EW(10832) = 0.435 + 0.412EW(10860)$. In the case of stars for which Figure 2 indicates that a telluric correction was needed to the He I *EW* measurements this correction was derived from the λ10860 line *EW* transformed via the relation shown in Figure 4. The value of $EW(10832)$ obtained in this way was subtracted from the measured He I *EW*. Corrections range from 41 mÅ for HD 23439B to 10 mÅ for HD 188510. Stars for which such a telluric correction has been applied are designated in Table 1. This technique has an advantage that the telluric correction is not estimated from hot star spectra obtained at a different time and place in the sky from the subdwarf observations.

For the star HD 103095, it is not the λ10832 telluric line that is a problem but another feature near 10825 Å. It is a very weak line and could only be measured cleanly in a few stars. This line was used in a similar manner to derive a telluric correction to the He I *EW* for HD 103095. The correction is small and amounts to 6 mÅ.

The resulting measurements of He I *EW* for each star in our program are listed in Table 1 and plotted against $(B - V)$ color and [Fe/H] abundance in Figures 5 and 6 respectively. There is little hint of any correlation between equivalent width and either $(B-V)$ color or [Fe/H] metallicity among the dwarfs. This conclusion is in accord with the findings of Takeda & Takada-Hidai (2011). Equivalent widths of the He I lines for HD 194598 and HD 201891 were measured by Takeda & Takada-Hidai (2011) based on observations obtained on 2009 July 29 and 30 (UT) with the Infrared Camera and Spectrograph on the Subaru telescope. They found a result of EW = 30.5 mÅ for HD 194598 compared with 27 mÅ from our NIRSPEC observations, and 26.2 mÅ for HD 201891 compared with 17 mÅ and 27 mÅ from the two NIRSPEC spectra. There is good consistency between the Keck and Subaru He I spectra for both of these stars. The equivalent widths for the dwarfs in the Takeda & Takada-Hidai (2011) sample range from 23-80 mÅ with the majority of their dwarfs being ∼ 23-45 mÅ. Thus the range in He I *EW* among the subdwarfs in the two investigations is quite similar.

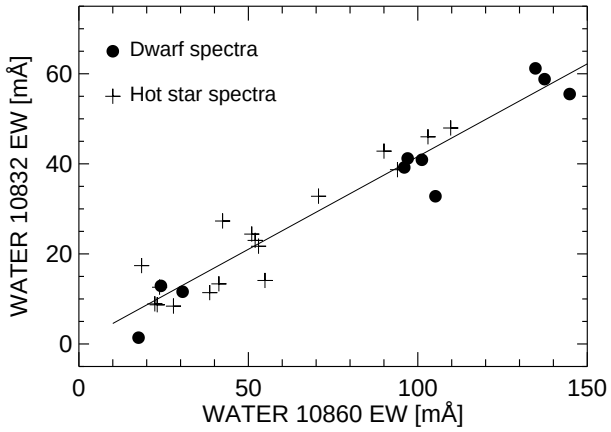

Figure 4. The equivalent width of the λ10832 telluric line versus the *EW* for the λ10860 telluric line. Filled circles and crosses denote measurements derived from spectra of subdwarf and hot stars respectively

By and large the equivalent widths of the He I line among the dwarfs are comparable to those exhibited by many (but not all) of the red giants and red horizontal branch (RHB) stars in the sample of Dupree et al. (2009). The largest equivalent widths (EW > 100 mÅ) found for some metal-poor giants and RHB stars by Dupree et al. (2009) are not present among the subdwarfs in our sample. However, many metal-poor giants in Dupree et al. (2009) do exhibit λ10830 equivalent widths of less than 70 mÅ, and overlap the range of *EW* seen among the subdwarfs in Figure 5.

A comparison can also be made between the metal-poor subdwarfs and Population I dwarfs. This is done in Figure 7 in which the He I *EW* is plotted versus $B - V$ for the metal-poor dwarfs from Table 1 and Population I dwarfs from two sources. The filled symbols denote subdwarfs from Table 1. The open circles denote the absorption equivalent widths of dwarf stars taken from Zarro & Zirin (1986) where the error bar represents their estimated measurement error from the spectra (having a resolution of R = 11000) for stars with equivalent

[3] IRAF is distributed by the National Optical Astronomy Observatories, which is operated by the Association of Universities for Research in Astronomy, Inc. under cooperative agreement with the National Science Foundation.

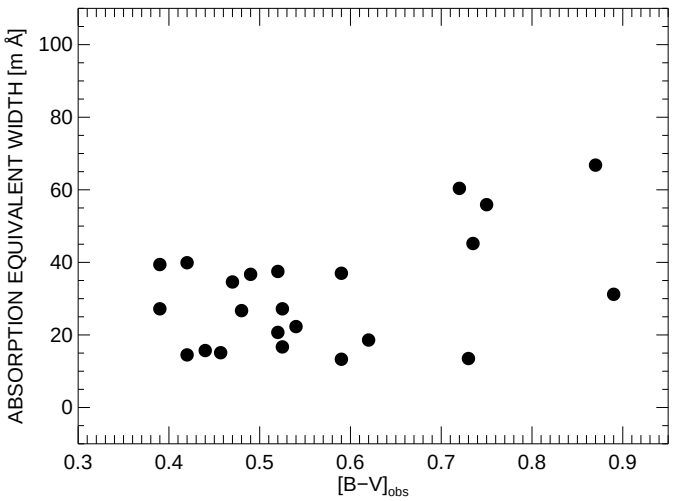

Figure 5. The equivalent width of the λ10830 He I line versus $(B-V)$ color for stars listed in Table 1.

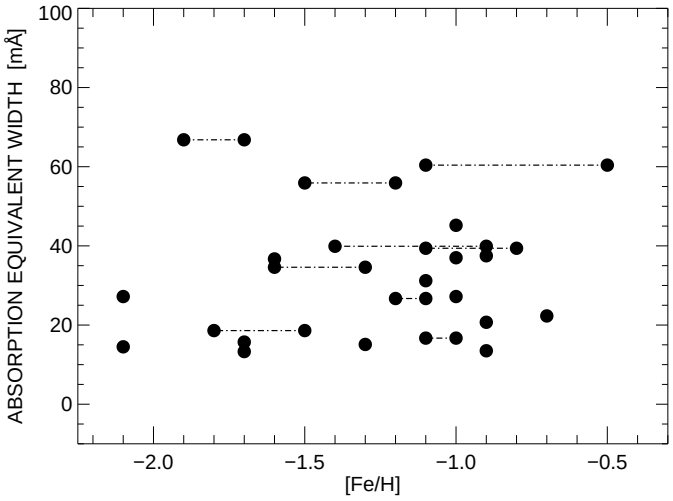

Figure 6. The equivalent width of the λ10830 He I line versus [Fe/H] metallicity for stars listed in Table 1. Where two different values of [Fe/H] are listed for a star in Table 1 a pair of points connected by a dashed line is plotted. Slight offsets in EW have been incorporated for clarity in display.

width less than 50 mÅ. The open square marks the value for the active dwarf ϵ Eri measured with a resolution of $R = 170,000$ from Sanz-Forcada & Dupree (2008). The variability is most likely real. The metal-poor subdwarfs have equivalent widths comparable to the weaker helium lines seen among dwarf stars of solar metallicity. There is a much greater range in EW among the Population I dwarfs, many of which have considerably stronger He I lines ($EW > 100$ m Å) than the subdwarfs.

In searching for evidence of an outflow one is looking for an asymmetric profile in which absorption exhibits a tail towards the Si I line at 10827 Å or a profile whose greatest depth is offset from the expected rest frame wavelength. Concerning line profile shapes, some dwarfs might show evidence for an asymmetric He I profile, including HD 23439B, HD 31128, HD 59374, HD 64606, HD 94028, HD 103095, and HD 221377. HD 64606 is problematic because of a telluric feature between the He I and Si I lines. HD 103095 shows a somewhat asymmetic profile but the line center is very close to the rest frame wavelength and the degree of extension toward the Si I line is modest. Possible blue-extended absorption in the case of both HD 23439B may be an artifact of incomplete continuum normalization since the line profile seems quite symmetric and the Si I line is quite broad with extensive wings on both blue and red sides.

Some metal-poor dwarfs do show possible evidence of He I line asymmetry and/or velocity shifts of the line core from the rest frame of the photosphere. Such cases are highlighted in column 11 of Table 1 with several annotations denoting either an asymmetric He I profile that is extended on the blue or red sides, or whether the deepest part of the line profile is offset from the expected restframe velocity, or whether emission appears to be present. In none of the spectra does the blue wing of the He I absorption line extend to the rest frame wavelength of the neighboring Si I line. In the case of five stars noted in Table 1 the possible presence of a telluric feature may be influencing the appearance of the line profile.

Various figures in Dupree et al. (1992), Smith et al. (2004), and Dupree et al. (2009) show examples of the types of fast outflow He I profiles that have been discovered among some Population II red giants. In such stars the broad He I absorption profile can extend blueward into the region of the 10827.1 Å Si I line. None of the subdwarf spectra in Figure 3 show the type of extended blue wing absorption seen in the field giants HD 6833 (Dupree et al. 1992) or HD 122563 (Smith et al. 2004) for example. As such, the metal-poor dwarfs do not show evidence for the type of high-speed outflows found among such metal-poor giants as HD 6833 (Dupree et al. 1992). Note this does not necessarily indicate that high speed flows are absent in these stars. High-velocity absorption arises in giants because the population in the metastable level spans an extended chromosphere allowing scattering of near-infrared photons and tracing the acceleration in the outflow. In contrast, the scale height of the atmosphere is less in dwarf stars than giants and helium would be present over a more narrow atmospheric region where the outflow velocity may be lower or nearly constant.

4. COMMENTS ON INDIVIDUAL STARS

Our general results have been presented in the preceding section. In this section comments about individual stars are given.

HD 7424. There is a difference of 0.6 dex in the [Fe/H] measurements of Peterson (1981) and Tomkin et al. (1992). The He I line may be blended with another very weak feature.

HD 59984 is considered to be a metal-poor disk dwarf and has been the subject of many metallicity measurements in addition to the work of Chen et al. (2000). The majority of the published values of [Fe/H] are close to -0.7 to -0.8 dex. It has a He I EW that is consistent with that of more metal-poor dwarfs of similar $(B-V)$ color that belong to the halo.

HD 64606 is listed as a spectroscopic binary in the catalog of Pourbaix et al. (2004) with a period of about 450 days. It was observed to exhibit Ca II H and K emission by Smith & Churchill (1998) with an asymmetry

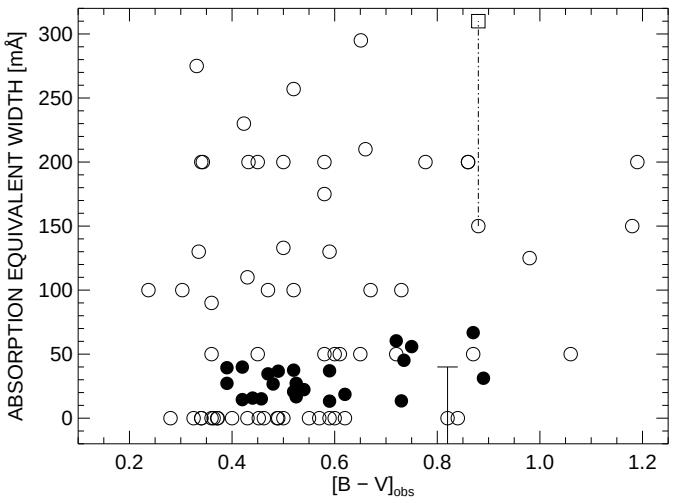

Figure 7. The equivalent width of the λ10830 He I line versus $(B-V)$ color for metal-poor subdwarfs stars listed in Table 1 (filled circles), as well as Population I dwarfs (open circles) from Zarro & Zirin (1986). The open square denotes a measurement for the star ϵ Eri obtained by Sanz-Forcada & Dupree et al. (2008).

parameter of $V/R > 1$, which is typical of other subdwarfs in their survey. HD 64606 was included in a search for X-ray activity among Population II field binaries by Ottman et al. (1997) using the *ROSAT* all-sky survey. The observations provided only an upper limit on any X-ray luminosity, this star was not among those Population II binaries detected by *ROSAT*. The He I line is relatively weak.

HD 23439B, HD 59374, HD 59984, HD 94028 and HD 97916. The possible asymmetries and/or wavelength offsets of the He I line noted in Table 1 for these stars may be influenced by the presence of a telluric feature.

5. DISCUSSION

The results of this work can be summarized as follows:
(i) Metal-poor field subdwarfs and dwarfs commonly exhibit a He I absorption line indicative of the presence of chromospheres.
(ii) The equivalent width of the He I absorption line is typically less than 70 mÅ among metal-poor dwarfs. Our results are consistent with the observations of Takeda & Takada-Hidai (2011) in this regard. The range of He I equivalent widths among the subdwarfs overlaps the range displayed by metal-poor red giants, however, some metal-poor giants do show notably stronger λ10830 lines.
(iii) There is no evidence in our data set for any correlation between He I line equivalent width and either [Fe/H] metallicity or $(B-V)$ color among metal-poor dwarf stars.
(iv) The dwarfs stars in our sample lack the strong EW > 100 mÅ absorption lines evident among some field RHB stars.
(v) Whereas some asymmetric profiles are discernible among metal-poor dwarfs, they generally do not display the type of high-speed blue-shifted outflow absorption found by Dupree et al. (1992, 2009) among some metal-poor red giants.

The process(es) responsible for populating the lower state of the 10830 Å triplet line have been the subject of debate (e.g., Zirin 1976, Cuntz & Luttermoser 1990; Sanz-Forcada & Dupree 2008). Among Population I dwarfs later than spectral type ∼ F7 there is a correlation between soft X-ray flux and the equivalent width of the He I λ10830 line (Zarro & Zirin 1986; Takeda & Takada-Hidai 2011). This correlation has been documented down to X-ray flux levels of $\log(f_{\rm x}/f_{\rm bol}) \sim -6.2$ at which the λ10830 equivalent width falls within the range $1.4 < \log EW < 2.0$ (see Fig. 5 of Takeda & Takada-Hidai 2011). Furthermore in the case of the Sun there are spatial correlations between the λ10830 line strength and X-ray and EUV flux (Harvey & Sheeley 1977; Thompson et al. 1993; Brajša et al. 1996). These correlations have been interpreted as resulting from photoionization of He I by X-rays followed by recombination to the triplet levels of neutral helium (e.g., Zirin 1975).

The most metal-poor halo dwarfs in Table 1 are presumably among the oldest stars in the Galaxy. As such their coronal activity is expected to have decreased to low levels. Such stars are expected to be considerably older than the Population I dwarfs in the Zarro & Zirin (1986) survey. Yet one can point to examples of metal-poor subdwarfs in Table 1 that have comparable He I EWs to some dwarfs in the Zarro & Zirin (1986) sample (Figure 7). Does this imply a decoupling of the He I line strength and coronal flux among dwarf stars of low levels of activity? Takeda & Takada-Hidai (2011) argued that the presence of He I equivalent widths of $1.0 < \log EW < 2.0$ among subdwarfs is consistent with old dwarf stars attaining a base level of activity that is driven by some heating mechanism that is unrelated to a magnetic dynamo. Since the He I λ10830 lower level is still being excited among Population II subdwarfs, if radiative excitation from high-energy coronal photons is the relevant mechanism then it might be expected that such stars should be detected in soft X-rays if deep enough integrations can be acquired by using orbiting X-ray observatories. However, none of the stars in Table 1 are found as detections in the *ROSAT All-Sky Survey Faint Source Catalogue* (Voges et al. 2000).[4]

The NIRSPEC spectra do not appear to have revealed any evidence among the subdwarfs in Table 1 for the fast ∼ 100 km s^{-1} outflows seen by Dupree et al. (1992, 2000) among some Population II red giants. This at least adds support to the suggestion that the fast winds seen in the He I profile are a by-product of red giant evolutionary processes. It is appropriate here to distinguish between an outflow (that is, a motion of material away from a star) and a wind (material exceeding the stellar escape velocity at a given radius). A notable distinction between the metal-poor red giants and the subdwarfs is not just the velocity of the outflow, but also that the subdwarfs have larger escape velocities. The data in this paper give no evidence that such outflowing material as is observed is unbound from the star, unlike the case for some red giants discussed by Dupree et al. (2009).

Among Population I giants of late-K spectral type O'Brien & Lambert (1986) and Lambert (1987) found

[4] Stellar metallicity might play a role here. Perhaps for a given energy input metal-poor atmospheres might be warmer than chromospheres of solar metallicity since they may not radiate as efficiently. If so, then higher chromospheric temperatures would increase the strength of the helium line.

evidence from the λ10830 profiles for time-variable mass motions in the chromosphere suggestive of "episodic ejection of matter and a subsequent return of some fraction of this matter to the photospheres in these stars." By contrast early-K Population I giants were found by them to have constant λ10830 profiles not dissimilar to that of the Sun. In the case of α Boo Lambert (1987) concluded that the profile variations may be periodic. Evidently when both Population I and II red giants evolve into the K spectral class dynamic phenomena become evident in the outer atmosphere. The challenge is to determine whether these outflows seen in the He I line are regular, semi-regular, or irregular, what the driving mechanism of the outflows is, and whether these mass motions trace significant episodes of mass loss, as argued by Dupree et al. (2009).

The authors wish to recognize and acknowledge the very significant cultural role and reverence that the summit of Mauna Kea has always had within the indigenous Hawaiian community. We are most fortunate to have the opportunity to conduct observations from this mountain. We thank the referee for useful comments on the paper.

REFERENCES

Abia, C., Rebolo, R., Beckman, J. E., & Crivellari, L. 1988, A&A, 206, 100
Andretta, V., & Giampapa, M. S. 1995, ApJ, 439, 405
Beers T.C., Chiba M., Yoshii Y., Platais I., Hanson R.B., Fuchs, B., & Rossi S. 2000, AJ, 119, 2866
Bond, H. E., & Luck, R. E. 1987, ApJ, 312, 203
Brajša, R., Pohjolainen, S., Ruždjak, V., Sakurai, T., Urpo, S., Vršnak, B., & Wöhl, H. 1996, SolPhys, 163, 79
Burris, D. L., Pilachowski, C.A., Armandroff, T.E., Sneden, C., Cowan, J.J., & Roe H. 2000, ApJ, 544, 302
Cacciari, C., Bragaglia, A., Rossetti, E., Fusi Pecci, F., Mulas, G., Carretta, E., Gratton, R. G., Momany, Y., & Pasquini, L. 2004, A&AS, 413, 343
Carney, B. W., Latham, D. W., Stefanik, R. P., Laird, J. B., & Morsem J. A. 2003, AJ, 125, 293
Casagrande, L., Schoenrich R., Asplund M., Cassisi S., Ramirez I., Melendez J., Bensby T., & Feltzing S. 2011, A&A, 530, 138
Cayrel de Strobel G., Soubiran C., & Ralite N. 2001, A&A, 373, 159
Chen, Y. Q., Nissen, P. E., Zhao, G., Zhang, H. W., & Benoni, T. 2000, A&AS, 141, 491
Clementini, G., Gratton, R. G., Carretta, E., & Sneden, C. 1999, MNRAS, 302, 22
Cuntz, M., & Luttermoser, D. G. 1990, ApJ, 353, L39
Dupree, A. K., Hartmann, L., & Smith, G. H. 1990, ApJ, 353, 623
Dupree, A. K., Li, T. Q., & Smith, G. H. 2007, AJ, 134, 1348
Dupree, A. K., Sasselov, D. D., & Lester, J. B. 1992, ApJ, 387, L85
Dupree, A. K., & Smith, G. H. 1995, AJ, 110, 405
Dupree, A. K., Smith, G. H., & Strader, J. 2009, AJ, 138, 1485
Dupree, A. K., Strader, J., & Smith, G. H. 2011, ApJ, 728, 155
ESA 1997, The Hipparcos and Tycho Catalogues, ESA SP-1200
For, B.-Q., & Sneden, S. 2010, AJ, 140, 1694
Fulbright, J. P. 2000, AJ, 120, 1841
Gratton, R. G., Sneden, C., Carretta, E., & Bragaglia, A. 2000, A&A, 354, 169
Harvey, J. W., & Sheeley, N. R. 1977, SolPhys, 54, 343
Lambert, D. L. 1987, ApJS, 65, 255
Lepine, S. 2007, AJ, 133, 889
Mauas, P. J. D., Cacciari, C., & Pasquini, L. 2006, A&AS, 454, 609
McLean, I. S., Graham, J. R., Becklin, E. E., Figer, D. E., Larkin, J. E., Levenson, N. A., & Teplitz, H. I. 2000, SPIE, 4008, 1048
McLean, I. S., McGovern, M. R., Burgasser, A. J., Kirkpatrick, J. D., Prato, L., & Kim, S. S. 2003, ApJ, 596, 561
McLean, I. S., et al. 1998, SPIE, 3354, 566
Mermilliod, J. -C., Mermilliod, M., & Hauck, B. 1997, A&AS, 124, 349
Mészáros, Sz., Dupree, A. K., & Szalai, T. 2009, AJ, 137, 4282
O'Brien, G. T. Jr., & Lambert, D. L. 1986, ApJS, 62, 899
Ottmann, R., Fleming, T. A., & Pasquini, L. 1997, A&A, 322, 785
Peterson, R. C. 1981, ApJ, 244, 989
Peterson, R. C., & Schrijver, C. J. 1997, ApJ, 480, L47
Peterson, R. C., & Schrijver, C. J. 2001, in 11th Cambridge Workshop on Cool Stars, Stellar Systems and the Sun, eds. R. J. Garcia Lopez, R. Rebolo, & M. R. Zapaterio Rosario (San Francisco: Astron. Soc. Pacific), p. 300
Pilachowski, C. A., Sneden, C., & Booth, J. 1993, ApJ, 407, 699
Pourbaix, D., et al. 2004, A&AS, 424, 727
Sanz-Forcada, J., & Dupree, A. K. 2008, A&A, 488, 715
Shcherbakov, A. G., & Shcherbakova, Z. A. 1991, in The Sun and Cool Stars. Activity, Magnetism, Dynamos. Proceedings of IAU Colloquium No. 130, eds. I. Tuominen, D. Moss, & G. Rudiger (Berline: Springer-Verlag), p. 252
Smith, G. H., & Churchill, C. W. 1998, MNRAS, 297, 388
Smith, G. H., & Dupree, G. H. 1998, AJ, 116, 931
Smith, G. H., Dupree, A. K., & Churchill, C. W. 1992, AJ, 104, 2005
Smith, G. H., Dupree, A. K., & Strader, J. 2004, PASP, 116, 819
Takeda, Y., & Takada-Hidai, M. 2011, PASJ, 63, S547
Thompson, W. T., Neupert, W. M., Jordan, S. D., Jones, H., Thomas, R. J., & Schmieder, B. 1993, SolPhys, 147, 29
Tomkin, J., & Lambert, D. L. 1999, 523, 234
Tomkin, J., Lemke, M., Lambert, D. L., & Sneden, C. 1992, AJ, 104, 1568
Vieytes, M., Mauas, P., Cacciari, C., Origlia, L., & Pancino, E. 2011, A&A, 526, 4
Voges, W., et al. 2000, VizieR Online Data Catalog, IX/29
Zarro, D. M., & Zirin, H. 1986,ApJ, 304, 365
Zirin, H. 1975, ApJL, 199, L63
Zirin, H. 1976, ApJ, 208, 414
Zirin, H. 1982, ApJ, 260, 655

Table 1
He I Line Characteristics of Metal-Poor Stars

HD (1)	Exp sec	V (3)	$B-V$ (4)	Par mas	M_V (6)	[Fe/H] (7)	[Fe/H] Ref	v_r km s^{-1}	EW(He) mÅ	Notes (11)
3179[a]	2×1×180	9.75	0.74	3.47	2.45	–1.0	a	–74	45.2	
3567	2×1×90	9.25	0.46	9.51	4.15	–1.3	c	–50	15.1	
7424	2×1×180	10.08	0.72	6.15	4.02	–0.5,–1.1	d,e	+85	60.4	
16031[b]	2×1×120	9.78	0.44	8.93	4.53	–1.7	c	+24	15.7	o?
23439B[b]	2×1×90	8.77	0.89	40.8	6.82	–1.1	f	+50	31.2	o?
25329	2×1×45	8.50	0.87	54.68	7.19	–1.7,–1.9	b,c	–30	66.8	
31128	2×2×(60+120)	9.13	0.49	15.0	5.01	–1.6	c	+105	36.7	o?
59374[b]	2×2×60	8.49	0.52	20.2	5.02	–0.9	c	+80	37.5	ar,o
59984[b]	2×1×60	5.90	0.54	35.82	3.67	–0.7	h	+55	22.3	ab,o
64090	2×2×60	8.30	0.62	34.3	5.98	–1.5,–1.8	b,c	–240	18.6	
64606[b]	2×2×15	7.44	0.73	49.78	5.93	–0.9	c	+93	13.5	
74000	2×2×180	9.67	0.42	7.86	4.15	–2.1	c	+204	14.5	
76932[b]	2×2×(5+5)	5.82	0.52	47.54	4.21	–0.9	c	+121	20.7	
84937	2×2×45	8.32	0.39	13.74	4.01	–2.1	c	–17	27.2	
94028[b]	2×1×100	8.23	0.47	21.11	4.85	–1.3,–1.6	i,c	+62	34.6	ab,o?
97916[b]	2×4×60	9.21	0.42	8.95	3.97	–0.9,–1.4	c,j	+55	39.9	ar
103095[b]	2×2×15	6.45	0.75	109.99	6.66	–1.2,–1.5	b,c	–98	55.9	ab
188510[b]	2×4×60	8.83	0.59	26.71	5.96	–1.7	c	–193	13.3	
194598	4×2×120	8.34	0.48	17.00	4.49	–1.1,–1.2	b,c	–246	26.7	
201889	2×3×45	8.06	0.59	18.60	4.41	–1.0	c	–103	37.0	
201891-1	2×1×45	7.37	0.53	29.10	4.69	–1.0,–1.1	b,c	–45	16.7	ab?
201891-2	2×3×25	....	....	.....	....	...		....	27.2	ab?
221377[b]	2×1×45	7.57	0.39	13.10	3.16	–0.8,–1.1	c,k	+27	39.4	ab,o

[a] Possibly a subgiant star on basis of position in the color-magnitude diagram of Figure 1
[b] The value of EW(He) have been corrected for a telluric feature as discussed in the text.

Reference key (column 8) for tabulated values of [Fe/H]:
(a) Burris et al. (2000)
(b) Gratton et al. (2000)
(c) Fulbright (2000)
(d) Peterson (1981)
(e) Tomkin et al. (1992)
(f) Tomkin & Lambert (1999)
(g) For & Sneden (2010)
(h) Chen et al. (2000)
(i) Clementini et al. (1999)
(j) Pilachowski et al. (1993)
(k) Abia et al. (1988)
Annotations in column 11: ab = a star with an asymmetric He I profile that is extended on the blue side; ar = a star with an asymmetric He I profile that is extended on the red side; o = a case where the deepest part of the line profile is offset from the expected restframe velocity; and em = emission.